Two- and Three-Dimensional Cloud-Resolving Model Simulations of the Mesoscale Enhancement of Surface Heat Fluxes by Precipitating Deep Convection

XIAOQING WU AND STEPHEN GUIMOND

Department of Geological and Atmospheric Sciences, Iowa State University, Ames, Iowa

(Manuscript received 27 September 2004, in final form 18 July 2005)

ABSTRACT

Two-dimensional (2D) and three-dimensional (3D) cloud-resolving model (CRM) simulations are conducted to quantify the enhancement of surface sensible and latent heat fluxes by tropical precipitating cloud systems for 20 days (10–30 December 1992) during the Tropical Ocean Global Atmosphere Coupled Ocean–Atmosphere Response Experiment (TOGA COARE). The mesoscale enhancement appears to be analogous across both 2D and 3D CRMs, with the enhancement for the sensible heat flux accounting for 17% of the total flux for each model and the enhancement for the latent heat flux representing 18% and 16% of the total flux for 2D and 3D CRMs, respectively. The convection-induced gustiness is mainly responsible for the enhancement observed in each model simulation. The parameterization schemes of the mesoscale enhancement by the gustiness in terms of convective updraft, downdraft, and precipitation, respectively, are examined using each version of the CRM. The scheme utilizing the precipitation was found to yield the most desirable estimations of the mean fluxes with the smallest rms error. The results together with previous findings from other studies suggest that the mesoscale enhancement of surface heat fluxes by the precipitating deep convection is a subgrid process apparent across various CRMs and is imperative to incorporate into general circulation models (GCMs) for improved climate simulation.

1. Introduction

Over the ocean surface, sensible and latent heat fluxes play a key role in regulating the atmospheric hydrological and energy cycle and account for nearly 30% of the mean annual global energy budget (Wallace and Hobbs 1977). General circulation models (GCMs) suffer adverse uncertainties in the coupling of the ocean–atmosphere system and surface energy budget that affect the credibility of information they provide (e.g., Godfrey and Lindstrom 1989; Godfrey et al. 1991). Cloud systems over the tropical oceans are known to be essential in assessing the surface energy balance through the modification of surface fluxes from mesoscale and cloud-scale motions, yet they remain subgrid scale in most GCMs. Observational studies using long-term surface meteorological data suggested that the enhancement of surface heat fluxes by atmospheric mesoscale systems can reach as high as 30% of the fluxes (e.g., Esbensen and Reynolds 1981; Liu 1988; Zhang 1995; Esbensen and McPhaden 1996). Parameterization and modeling studies showed that both boundary layer free convection and precipitating deep convection can result in the mesoscale enhancement of surface fluxes through the horizontal wind variability, that is, the convection-induced gustiness at the surface (e.g., Godfrey and Beljaars 1991; Jabouille et al. 1996; Mondon and Redelsperger 1998; Redelsperger et al. 2000). However, the mesoscale enhancement of the surface heat fluxes has not been incorporated into most GCMs although the GCM studies (e.g., Miller et al. 1992) demonstrated that the simulation of tropical circulation is sensitive to the parameterization of surface fluxes under low surface wind conditions.

The Tropical Ocean Global Atmosphere Coupled Ocean–Atmosphere Response Experiment (TOGA COARE; e.g., Webster and Lukas 1992; Godfrey et al. 1998) and the development of cloud-resolving models (CRMs) in the last decade provided a unique opportunity to quantify the mesoscale enhancement of surface heat fluxes. The domain of TOGA COARE, in the western Pacific warm pool, is characterized by high sea surface temperatures (SSTs; ~30°C) and strong

Corresponding author address: Dr. Xiaoqing Wu, Department of Geological and Atmospheric Sciences, Iowa State University, Ames, IA 50011.
E-mail: wuxq@iastate.edu

convective events that make it suitable for a detailed, albeit complex, analysis of the ocean–atmosphere system. CRMs, which explicitly resolve convection and mesoscale organization, can produce fine spatial and temporal distribution of cloud-scale properties in large domains (1000s km) and for long periods (several months) when forced by the objectively analyzed evolving large-scale advection and wind fields obtained from field experiments (e.g., Grabowski et al. 1996, 1998; Wu and Moncrieff 1996). Jabouille et al. (1996) used a three-dimensional (3D) CRM developed by Redelsperger and Sommeria (1986) to simulate two convective cases (each lasts less than a day) observed during TOGA COARE and demonstrated an enhancement of the surface heat fluxes by a factor of 2 in the precipitating region due to the intense wind gusts. Redelsperger et al. (2000) applied a similar analysis to two multiday two-dimensional (2D) simulations of free convection in undisturbed conditions and precipitating deep convection during TOGA COARE. A parameterization of mesoscale enhancement of surface fluxes was developed for each type of convection by representing the convection-induced gustiness in terms of convective properties such as free convection velocity, downdrafts, updrafts, and precipitation.

The objective of this paper is to assess the efficiency of 2D and 3D versions of the CRM in quantifying the mesoscale enhancement of surface sensible and latent heat fluxes by precipitating deep convection over the tropical Pacific Ocean. Month-long 2D CRM simulations of TOGA COARE cloud systems were performed and extensively evaluated against various independent datasets such as outgoing longwave radiative (OLR) flux, albedo, cloud radiative forcing, surface sensible and latent heat fluxes, airborne radar reflectivity, and rainfall measurements (e.g., Wu et al. 1998, 1999; Wu and Moncrieff 2001). For the purpose of this study, we conducted both 2D and 3D CRM simulations for a period of 20 days (10–30 December) during TOGA COARE. With the CRM-produced cloud-scale properties such as temperature, moisture, and wind fields, a diagnostic analysis is performed to quantify the enhancement of surface heat fluxes. In addition, the precipitation parameterization developed by Redelsperger et al. (2000) is evaluated for each version of the CRM. Recently, Grabowski (2001) and Randall et al. (2003) proposed a methodology for the representation of convection and clouds in climate by inserting the framework of a CRM into each GCM grid box. The so-called "superparameterization" explicitly allows the coupling of simulated cloud processes (e.g., deep convection, cloud overlap, and enhancement of surface fluxes) on local scales from the CRM with the large-scale dynamics of GCMs. The use of a 3D CRM at each grid point in a GCM is much too expensive, and therefore superparameterizations mainly utilize 2D CRMs. The present study will determine the dimensionality (2D or 3D) of the CRM best suited for inclusion into a GCM in the context of mesoscale enhancement of surface heat fluxes by precipitating deep convection.

The organization of this paper is as follows. In the next section, the CRM used in this study will be briefly described along with the design of the experiment including both 2D and 3D frameworks. In section 3, the analysis of the mesoscale enhancement of surface fluxes will be provided with the definition of enhancement as well as an examination of enhancement for two snapshots of precipitating convection during TOGA COARE. Section 4 will contain a meticulous comparison of results obtained utilizing 2D and 3D CRMs. Finally, in section 5 conclusions will be offered.

2. Cloud-resolving model and experimental design

The cloud-resolving model used in this study is the Iowa State University (ISU) CRM, which is based on the Clark–Hall model (Clark et al. 1996). The cloud dynamics is a finite-difference formulation of the anelastic and nonhydrostatic equations. The microphysical processes are represented by the Kessler (1969) bulk warm rain parameterization and the Koenig and Murray (1976) bulk ice parameterization. The radiative processes are treated by the National Center for Atmospheric Research (NCAR) Community Climate Model version 3 (CCM3) radiation scheme (Kiehl et al. 1996). The surface sensible and latent heat fluxes are parameterized by a simplified form of the TOGA COARE surface flux algorithm (Fairall et al. 1996; Wu et al. 1998). Periodic lateral boundary conditions are used to facilitate a mathematically consistent framework such that no domain-averaged vertical velocity is present except from the large-scale forcing (Grabowski et al. 1996).

The evolving large-scale vertical and horizontal advection obtained during TOGA COARE is added to the temperature and moisture equations. Since the large-scale forcing for the horizontal wind field (especially the large-scale pressure gradient) is difficult to obtain from observations, a relaxation term is included in the momentum equations. This is the simplest way to emulate the control of the cloud system dynamics by the observed large-scale momentum and shear (e.g., Grabowski et al. 1996; Wu et al. 1998). The domain-averaged zonal and meridional winds are thereby constrained to follow the observed values. A detailed discussion of the way through which the CRM is forced by

observed large-scale conditions is presented in Grabowski et al. (1996).

For 2D simulations, the domain is 840 km long with a horizontal resolution of 3 km and is 40 km deep with 52 levels in a stretched grid (100 m at the surface, increasing to 1500 m at the top of the domain). The model is aligned east–west in the two-dimensional x–z. A time step of 15 s is used. Free-slip, rigid-bottom, and top boundary conditions are applied together with a gravity wave absorber in the uppermost 14 km of the domain. Radiation calculations are performed every 600 s while the most recent tendencies were applied between consecutive radiation calculations. For 3D simulations, the horizontal domain is 840 km $\times$ 840 km with a 3-km resolution. There are 52 levels in the vertical with a stretched grid as in 2D simulations. The bottom, top, and lateral boundary conditions are the same as the 2D setup.

Both 2D and 3D simulations are performed for 20 days from 10 to 30 December 1992. The evolving large-scale profiles of temperature, moisture, winds, and advective tendencies of temperature and moisture were averaged over the Intensive Flux Array (IFA; Lin and Johnson 1996). The IFA domain measures about 700 km in the east–west direction (151°–158°E) and about 500 km south–north (4°S–1°N). The averaged SST data over the IFA were calculated from four buoy datasets; namely, one Improved Meteorological (IMET) surface mooring and three TOGA Tropical Atmosphere Ocean (TAO) Automated Temperature Line Acquisition System (ATLAS) moorings. During the period, episodes of very strong cooling and moistening were present over the IFA, and easterlies were slowly giving way to westerlies (Wu et al. 1998). The low-level wind shear was enhanced below 3 km after 20 December. As the westerly winds increased to their maximum speed and depth (27–30 December), the magnitude and duration of the large-scale cooling and moistening was significantly decreased. The SST was decreasing during the period and the amplitude of the diurnal cycle was considerably smaller, apart from days 15, 18, and 19 when only a few clouds occurred in satellite pictures.

3. Comparison of mesoscale enhancement in 2D and 3D CRM simulations

a. Definition of enhancement

The mesoscale enhancement of fluxes can be estimated by the diagnostic calculation of surface heat fluxes using the CRM-produced cloud-scale variables including temperature, moisture, and wind fields (e.g., Jabouille et al. 1996; Redelsperger et al. 2000). In the control CRM simulations, the surface flux at each grid point is calculated by the TOGA COARE flux algorithm (Fairall et al. 1996), that is,

$$F_i = -\alpha_i(X_i - X_s)U_i, \tag{1}$$

where F_i is the surface flux for either sensible or latent heat; U_i and X_i are the wind speed and the transported variable (temperature for sensible heat flux and water vapor mixing ratio for latent heat flux) at the first model level (50 m), respectively; X_s is the observed sea surface temperature and water vapor mixing ratio; and α_i is the bulk transfer coefficient dependent on stability of the atmosphere and roughness length. The domain-averaged heat flux from the CRM approach, which will be referred to as the "control flux" in this paper, is simply

$$\overline{F} = \frac{1}{N}\sum_i F_i, \tag{2}$$

where N is the total grid points (280 in 2D model and 280 $\times$ 280 in 3D model).

In the diagnostic calculation of surface heat fluxes, instead of calculating the flux at each grid point of the CRM, the domain mean heat flux is computed only once for each time step by the TOGA COARE flux algorithm

$$\hat{F} = -\hat{\alpha}(X_D - X_s)U_D, \tag{3}$$

where $U_D = \sqrt{u_D^2 + v_D^2}$ is the wind speed; $u_D = (1/N\Sigma_i u_i)$ and $v_D = (1/N\Sigma_i v_i)$ are domain-averaged zonal and meridional wind components, respectively; X_D is the domain-averaged temperature or water vapor mixing ratio; and $\hat{\alpha}$ is the bulk transfer coefficient. This formulation for surface fluxes is similar to that used in GCMs where X_D, u_D, and v_D are grid-scale temperature, moisture, and zonal and meridional wind components. The flux from the diagnostic calculation or the GCM approach will be termed as "average flux" in this paper. The nonlinear correlation between subgrid wind, temperature, and moisture variability is not included in the calculation of average flux.

The difference ΔF of $\overline{F}$ and $\hat{F}$ is referred to as the mesoscale enhancement of surface fluxes for sensible or latent heat by precipitating deep convection in this study. Convective events that are associated with periods of precipitation, updrafts, and downdrafts can significantly enhance the sensible and latent heat fluxes through the increase in wind speeds associated with precipitating events as well as the decrease in air temperature in the rainfall region (e.g., Jabouille et al. 1996; Redelsperger et al. 2000). It was shown by previous studies that differences between the domain-averaged wind speed $\overline{U} = (1/N\Sigma_i\sqrt{u_i^2 + v_i^2})$ over all

grid points and the wind speed U_D of domain-averaged zonal and meridional components are the main contributor to the mesoscale enhancement. Since U_D is smaller than or equal to $\overline{U}$ due to the subgrid variability of wind components under the convective situation, a gustiness velocity U_g can be used to measure the impact of variability on the domain-averaged wind speed, that is,

$$\overline{U}^2 = U_D{}^2 + U_g{}^2. \tag{4}$$

Because the convection-induced gustiness is a subgrid process in GCMs, its parameterization in terms of convective properties has been proposed and derived from the CRM simulations. This relationship will be investigated using both 20-day 2D and 3D CRM simulations of TOGA COARE cloud systems.

b. *Mesoscale enhancement by CRM-simulated TOGA COARE cloud systems*

The TOGA COARE experiment is particularly interesting because it contains periods of intense convective activity that allow for a detailed discussion on the enhancement defined above. Figures 1 and 2 exhibit the time series of sensible and latent heat fluxes for the 2D and 3D from the CRM and GCM approach, respectively. Both 2D and 3D evolutions of the enhancement are remarkably similar with the enhancement in the first 10 days larger than the second 10 days. Consistent with previous CRM studies (e.g., Redelsperger et al. 2000), the evolution of differences between control flux and average flux correlates well to that of differences between the domain-averaged wind speed $\overline{U}$ and the wind speed U_D in Fig. 3. The relationship between the enhancement of surface fluxes and the gustiness (horizontal wind variations) U_g can be better viewed from the scattered plot of 6-hourly averages in Fig. 4, which shows mostly positive correlation between the two except few small negative enhancements for small U_g. In general, the small U_g is mostly associated with the large wind speed and scattered convection, and the average flux may be slightly larger than the control flux because of the nonlinearity throughout the iterations in getting the bulk transfer coefficients. Peaks in the surface precipitation time series for both 2D and 3D CRMs (Figs. 5a,b) also correspond to large values of the enhancement, although not as significant as the gustiness, as noted from the scattered plots of 6-hourly averages in Figs. 6a,b.

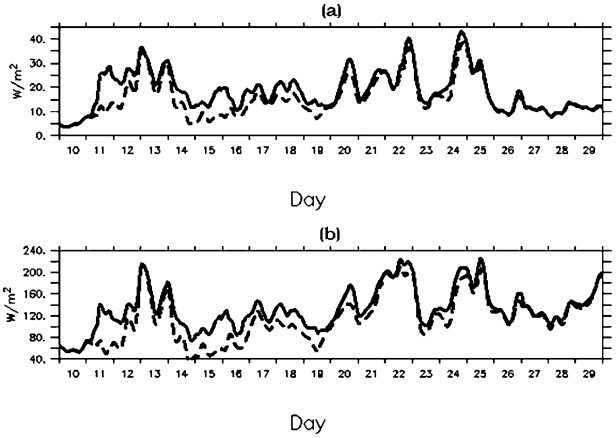

FIG. 2. Same as in Fig. 1, but using the 3D CRM.

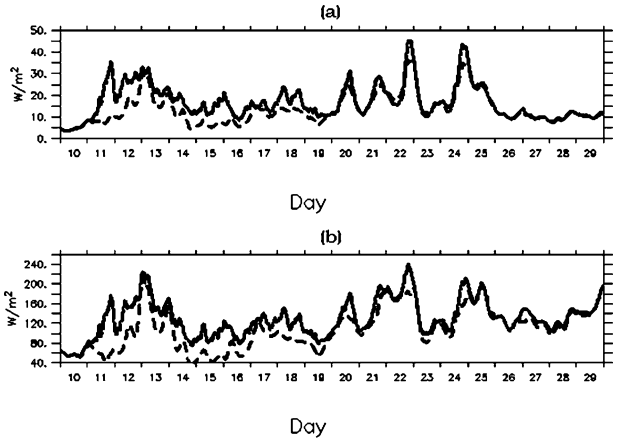

FIG. 1. Time series of surface (a) sensible and (b) latent heat fluxes with a 15-min step using the 2D CRM during the TOGA COARE. In each plot, solid curves represent the control flux from the CRM approach and dashed curves the average flux from the GCM approach.

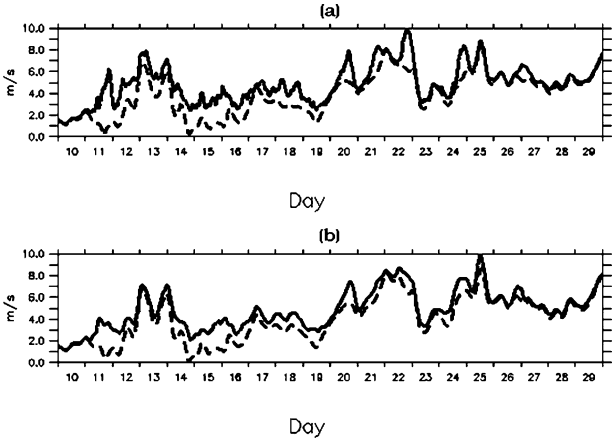

FIG. 3. Time series of the horizontal wind speeds from (a) 2D CRM and (b) 3D CRM with a 15-min step during the TOGA COARE. In each plot, solid curves represent the domain-averaged wind speed $\overline{U}$and dashed curves the wind speed U_D of domain-averaged zonal and meridional components.

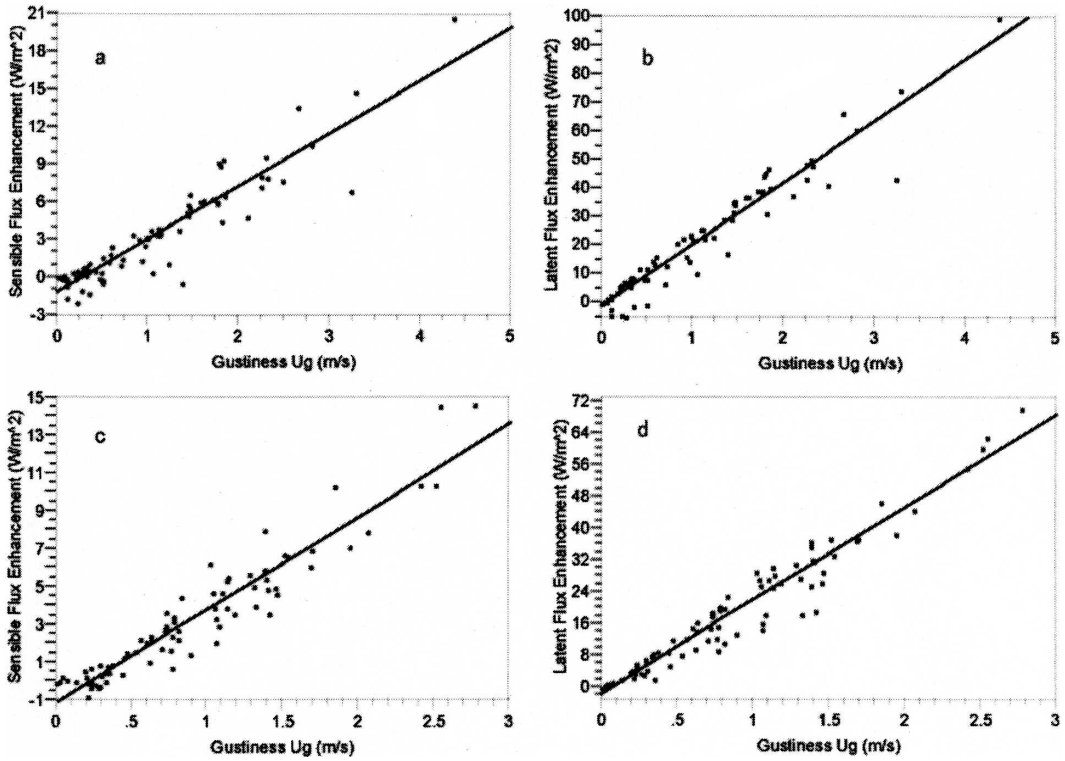

FIG. 4. Scatterplots with linear regressions of the mesoscale enhancement of 6-hourly surface sensible and latent heat fluxes vs gustiness speed U_g from the (a), (b) 2D CRM and (c), (d) 3D CRM for 10–30 Dec 1992.

Table 1 shows the mean percentages of enhancement for both the sensible and latent heat fluxes for 2D and 3D CRMs as well as the mean values of enhancement calculated during the TOGA COARE period. The mean percentages as well as the mean values of the mesoscale enhancement for the total sensible heat flux are found to be nearly the same for both 2D and 3D CRMs. Similar results are found for the total latent heat flux with both 2D and 3D CRMs yielding a mean percentage of enhancement within 2% and a mean value within 2.4 W m^{-2} of the other model. Results from Esbensen and McPhaden (1996) for surface fluxes averaged over a longer time span in the equatorial Pacific (1991–94 rainy season) show similar values to the fluxes calculated herein with the enhancement representing 17% of the mean for the sensible flux and 15% of the mean for the latent flux. Data interpreted from Redelsperger et al. (2000) during two shorter periods of TOGA COARE (10–17 December and 20–26 December 1992) reveal that approximately 25% of the total sensible heat flux and 24% of the total latent heat flux can be explained by the mesoscale enhancement.

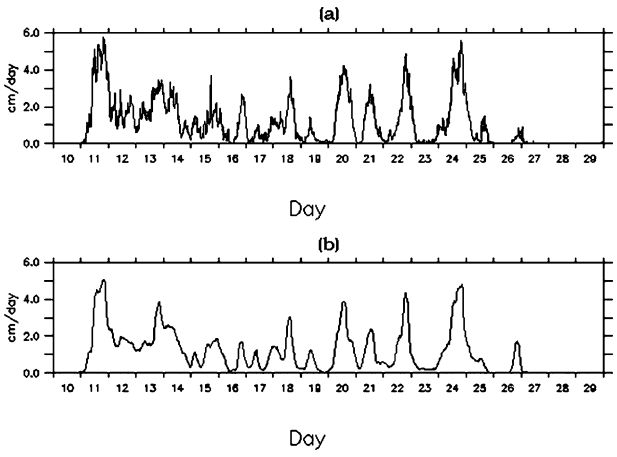

FIG. 5. Time series of the surface precipitation from the (a) 2D CRM and (b) 3D CRM with a 15-min step during the TOGA COARE.

c. *Case studies of mesoscale enhancement and sensitivity experiments of 2D CRM*

To facilitate an understanding of the reasons behind the enhancement of the surfaces heat fluxes in one region and nonenhancement in another, two snapshots were analyzed from the 2D CRM simulations. The first case was analyzed at 1200 UTC 11 December 1992, which is characterized by strong convection and signifi-

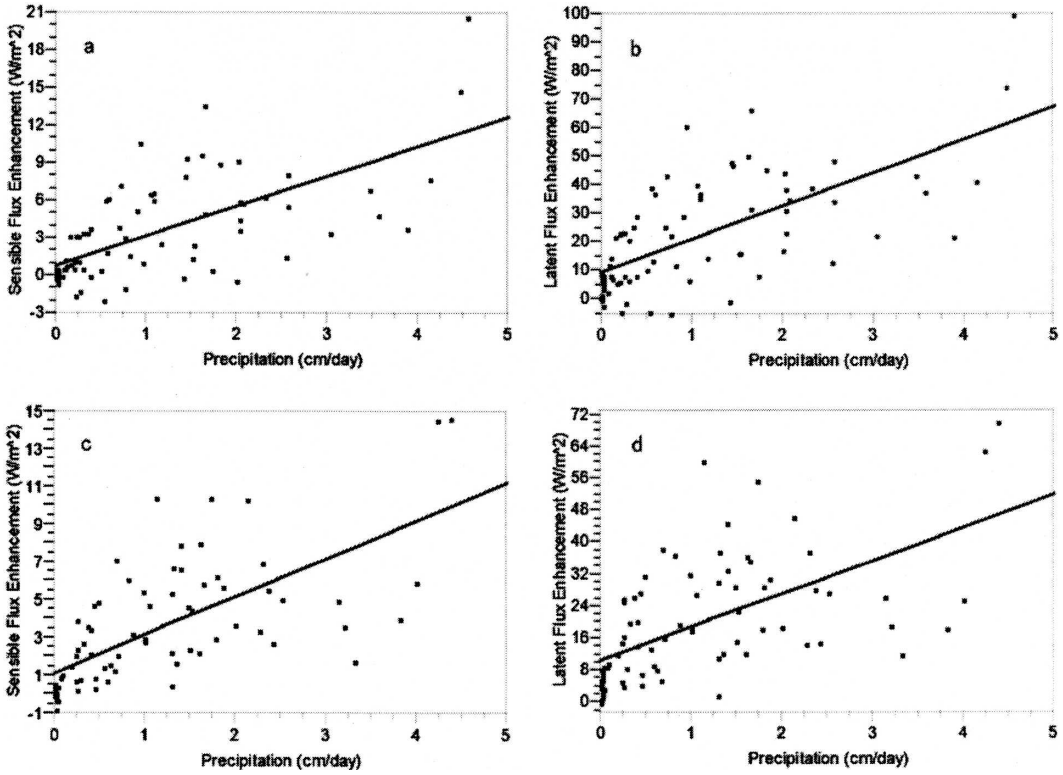

FIG. 6. Same as in Fig. 4, but for precipitation.

cant mesoscale enhancement. The second case was analyzed at 1200 UTC 20 December 1992, which is featured by pronounced convection, but with very minimal mesoscale enhancement. The CRM defines a grid point as being cloudy if the total condensate (the sum of liquid and ice water mixing ratios) is greater than or equal to 0.1 g kg^{-1} (Wu et al. 1998). This technique was applied to the data of the time period in question to analyze the strength and development of convection and their subsequent modification of surface fluxes. Figure 7a for the first case shows values of total condensate greater than 5 g kg^{-1} within an extensive depth of the lower atmosphere (from 3 to 13 km) with the cloud top stretching up around 16 km. The corresponding plot of horizontal wind speeds (Fig. 7b) exhibits turbulent fluctuations of the winds from positive to negative values indicating west and east winds, respectively in the regions of convective clouds. The mean wind speed over the domain is 0.95 m s^{-1} and the mesoscale enhancements are 50% and 45% for sensible and latent heat fluxes, respectively. Figure 8a from the second case shows a broader range of convective activity with roughly two distinct regions of total condensate including values in the range of 2–3 g kg^{-1}. The corresponding plot of horizontal wind speeds (Fig. 8b) shows large positive values of the wind in cohesion with the presence of a westerly wind burst (WWB) in this time period. The mean wind speed is 4.67 m s^{-1}, and the enhancements are 7% and 11% for sensible and latent heat fluxes, respectively. These results clearly demonstrate that under the condition of low mean wind speed over the domain, convective processes can significantly enhance the surface heat fluxes.

TABLE 1. Twenty-day (10–30 Dec 1992) mesoscale enhancement of sensible and latent heat fluxes by precipitating deep convection in terms of percentage and mean (W m^{-2} from 2D and 3D CRM simulations.

	Sensible flux		Latent flux	
Enhancement	%	Mean (W m^{-2})	%	Mean (W m^{-2})
2D CRM	17	3.28	18	21.68
3D CRM	17	3.26	16	19.29

Several 2D simulations are performed to examine the sensitivity of mesoscale enhancement of fluxes to the grid resolution and domain size. With the same domain size of 840 km but the finer resolution of 1 km than the control run, the 20-day mean enhancement decreases less than 2%. To address the dependence of flux en-

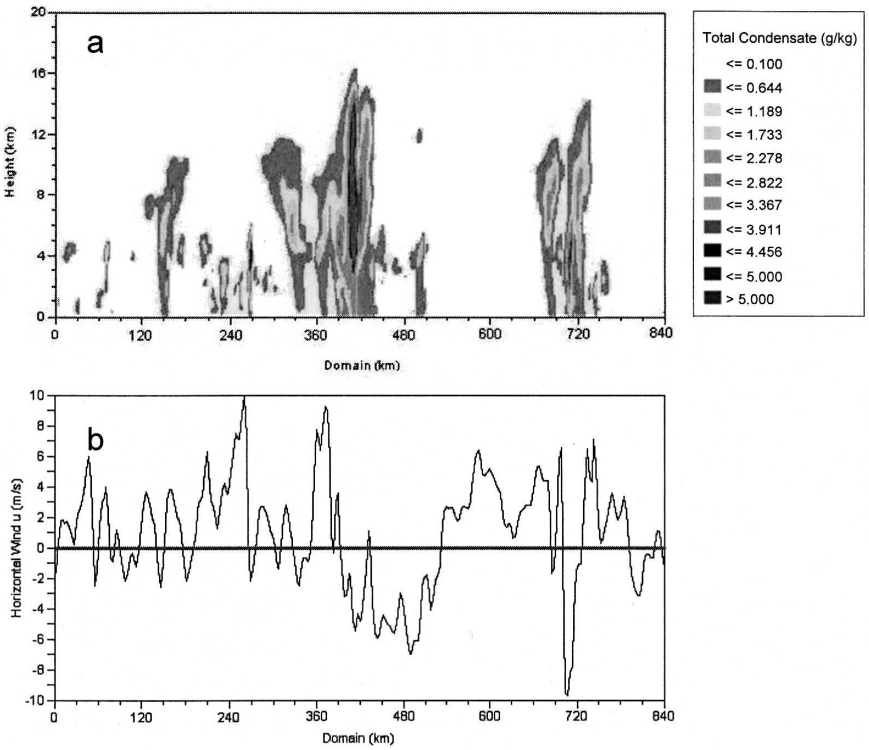

FIG. 7. (a) Vertical cross section of total condensate mixing ratio (g kg^{-1}) and (b) the corresponding surface horizontal wind speed (m s^{-1}) over the 2D CRM domain for 1200 UTC 11 Dec 1992.

hancement on the domain size (or the resolution of GCMs), another 2D simulation with the resolution of 1 km but the domain size of 280 km was performed and the 20-day mean enhancement decreases 5% compared to the 2D run with the same resolution of 1 km but the domain size of 840 km. The decrease of flux enhancements is largely due to the smaller wind variability over the smaller domain.

4. Parameterization of mesoscale enhancement

Horizontally homogeneous parameters over a GCM grid box will not suffice in getting accurate surface heat fluxes when subgrid scale motions induced by convective events are occurring. Several studies have proposed to include the mesoscale enhancement in the flux calculation by parameterizing the convection-induced gustiness as a function of convective cloud properties such as the precipitation and cloud mass fluxes (e.g., Jabouille et al. 1996; Zulauf and Krueger 1997). Work completed by Redelsperger et al. (2000) using a fit to a logarithmic function relating the gustiness to cloud properties yields a general form of the equation

$$U_g = \log(A + Bx - Cx^2), \tag{5}$$

where A, B, and C are coefficients; x is the cloud variable in question; and U_g is the gustiness factor in meters per second. By applying a least squares fit to x through (5), one can solve for values of A, B, and C. In this study, a quadratic fit with intercept constrained to 1.0 was performed in order to yield values for B and C. Applying a constant gustiness U_g of 3 m s^{-1} to the fluxes recovered the control fluxes rather well, but the lack of time variation resulted in high root-mean-square (rms) errors for the heat fluxes using both 2D and 3D CRMs as is seen in Table 2.

Upon applying the method described in the previous section, it was found that the coefficients outlined by Redelsperger et al. (2000) for the precipitation parameterization performed the most desirable results for the gustiness calculation using both 2D and 3D CRMs. This formulation gives

$$U_g = \log(1.0 + 6.69P - 0.476P^2), \tag{6}$$

where P is precipitation in centimeters per day. Figure 9 depicts the approximation of the mesoscale enhancement through the precipitation parameterization for sensible and latent heat fluxes using both 2D and 3D models. The precipitation scheme from the 2D CRM

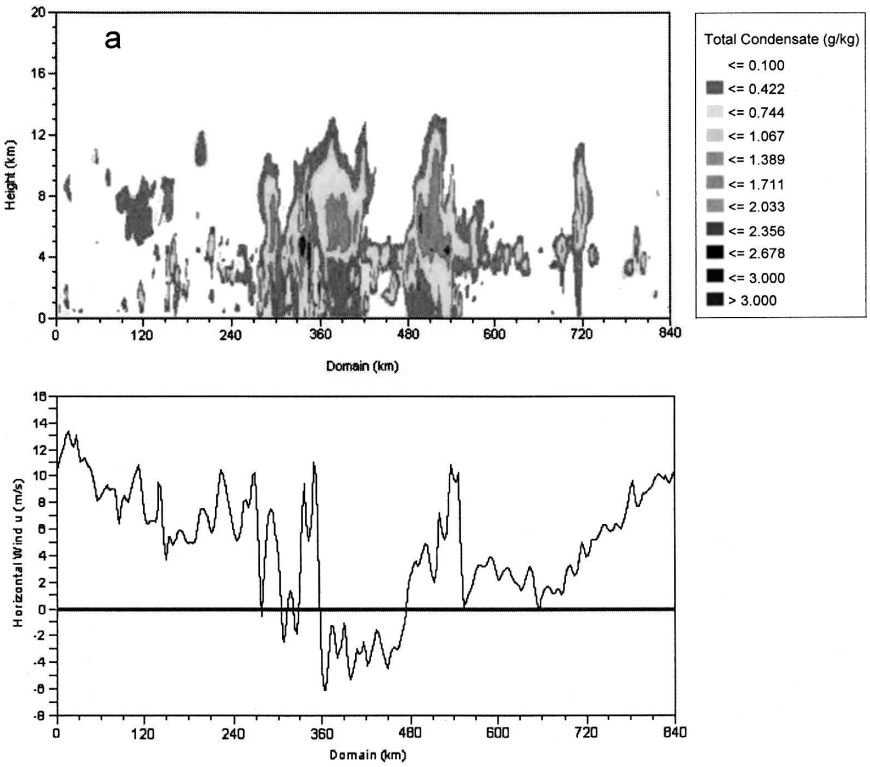

FIG. 8. Same as in Fig. 7, but for 1200 UTC 20 Dec 1992.

produces a reduction in rms error quite similar to the 3D for the sensible heat flux (1.65 and 1.87 W m^{-2}, respectively) and the latent heat flux (6.40 and 6.81 W m^{-2}, respectively) as seen in Table 2. The precipitation representation recovers the mean fluxes rather well for the sensible heat flux but leaves room for improvement in the latent heat flux, especially with the 2D CRM. The correlation coefficients for the 3D CRM are found to be more significant than the 2D for the precipitation scheme shown in the statistical summary in Table 2.

To calculate the cloud mass fluxes, a similar technique to the total condensate mixing ratio was used to resolve updrafts and downdrafts. At levels where the total condensate is larger than or equal to 0.1 g kg^{-1},

TABLE 2. Twenty-day mean and std dev of surface sensible and latent heat fluxes (W m^{-2}) from control simulations, diagnostic analyses, and four different parameterizations of gustiness for 2D and 3D CRMs. The rms error and correlation coefficient (r) from 2D and 3D control simulations are also included.

Surface flux		Sensible				Latent			
CRM	Method	Mean	Std dev	Rms	r	Mean	Std dev	Rms	r
2D	Control	16.9	8.0	0.00	1.00	130.0	37.1	0.00	1.00
	Average	13.6	7.0	4.31	0.84	108.3	41.7	19.09	0.86
	$U_g = 3$	17.5	6.6	2.67	0.94	135.6	32.2	16.95	0.89
	$U_g = f(P)$	15.4	7.5	2.66	0.94	119.1	38.7	12.69	0.94
	$U_g = f(M_u)$	14.8	7.1	3.51	0.90	116.2	39.6	16.88	0.89
	$U_g = f(M_d)$	14.9	7.6	3.17	0.92	116.3	40.2	15.37	0.91
3D	Control	18.4	8.2	0.00	1.00	132.5	38.7	0.00	1.00
	Average	15.2	7.7	3.38	0.91	113.2	43.8	13.87	0.93
	$U_g = 3$	19.3	7.2	1.60	0.98	140.4	33.7	11.11	0.96
	$U_g = f(P)$	17.2	8.1	1.51	0.98	124.4	40.8	7.06	0.98
	$U_g = f(M_u)$	16.0	7.8	2.44	0.95	117.8	42.2	10.34	0.96
	$U_g = f(M_d)$	16.0	7.8	2.36	0.96	117.8	42.1	10.07	0.97

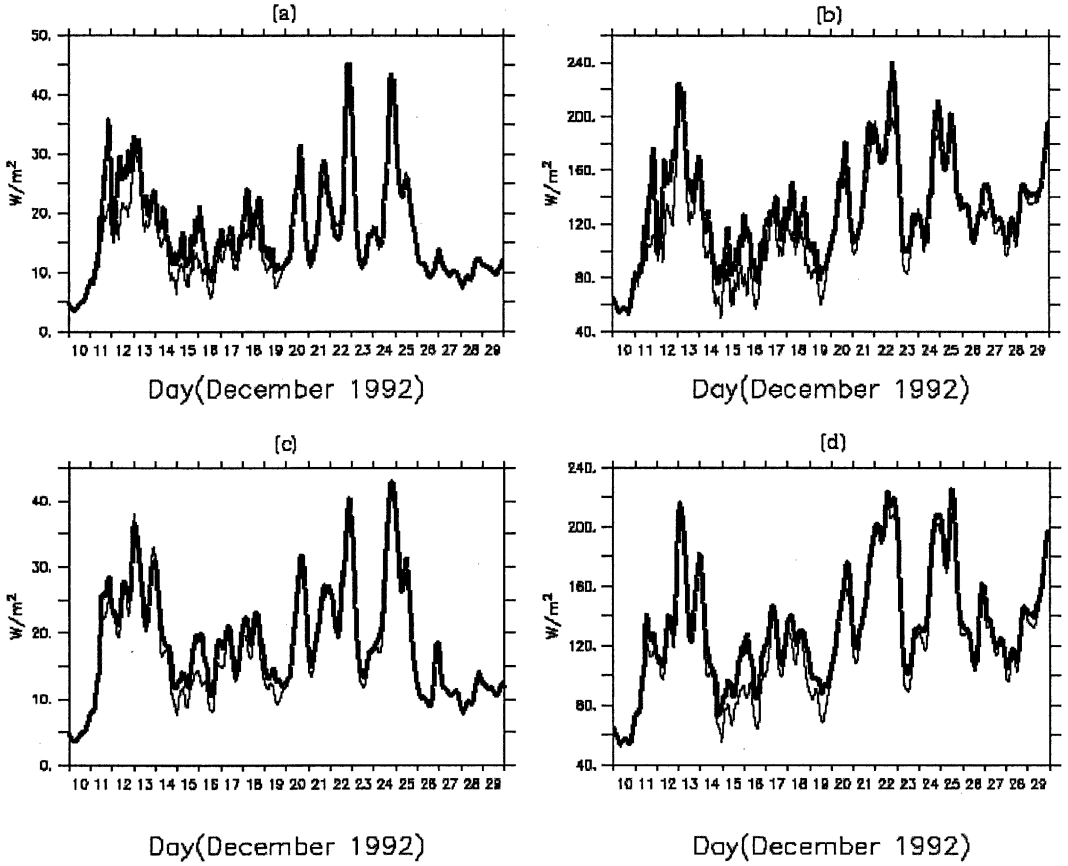

FIG. 9. Comparison of the time series of surface heat fluxes with a 15-min step during the TOGA COARE. (a) Sensible and (b) latent fluxes for the 2D CRM, and the (c) sensible and (d) latent fluxes for the 3D CRM. In each figure, the thick curve represents the control flux and the thin curve portrays the parameterization using the precipitation [Eq. (6)].

the updraft and downdraft cloud mass fluxes were calculated and then averaged over the domain for each level (Wu et al. 1998). To determine cloud-base level, the first level having an updraft or downdraft flux not equal to zero was used and the corresponding value calculated. The parameterization of gustiness in terms of cloud mass fluxes provided by Redelsperger et al. (2000) did not perform as well in this scenario because of the differences in their CRM's treatment of cloud microphysics and determination of cloud-base level. Using 2D and 3D CRM simulations presented in the last section, two parameterizations were derived in terms of the updraft and downdraft mass fluxes. The formulated functions follow:

2D CRM (updraft)

$$U_g = \log(1.0 + 9.68M_u - 3.21M_u^2), \quad (7)$$

3D CRM (updraft)

$$U_g = \log(1.0 + 3.73M_u - 0.61M_u^2), \quad (8)$$

2D CRM (downdraft)

$$U_g = \log(1.0 + 0.64M_d + 15.04M_d^2), \quad (9)$$

3D CRM (downdraft)

$$U_g = \log(1.0 - 1.76M_d + 0.10M_d^2), \quad (10)$$

where M_u and M_d are the updraft and downdraft cloud mass fluxes in mb hour^{-1}, respectively. The updraft scheme from the 2D CRM produces a reduction in rms error similar to the 3D CRM for the sensible flux (0.80 and 0.94 W m^{-2}) and the latent heat flux (2.21 and 3.53 W m^{-2}). Figure 10 outlines the performance of the downdraft scheme for the latent heat flux using both the 2D and 3D CRMs. The downdraft parameterization yields a reduction in rms error roughly similar to the updraft scheme, and across each model, they remain nearly identical for the sensible flux (1.14 and 1.02 W m^{-2} for 2D and 3D, respectively) and the latent heat flux (3.72 and 3.80 W m^{-2}). Both cloud mass flux representations equally recover the mean fluxes indicating

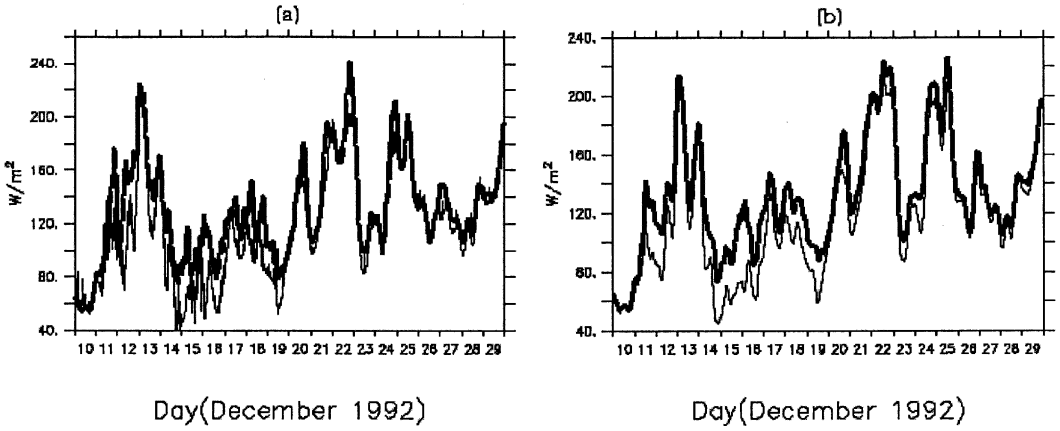

FIG. 10. Comparison of the time series of surface heat fluxes with a 15-min step during the TOGA COARE. Latent heat flux from the (a) 2D and (b) 3D CRM. In each figure, the thick curve represents the control flux and the thin curve depicts the parameterization using the downdraft mass flux [Eqs. (9) and (10)].

that the results are indistinguishable in this context. Finally, it is noted from Table 2 that the correlation coefficients between the parameterized surface heat fluxes and the control fluxes are higher in the 3D than the 2D.

5. Conclusions

General circulation models (GCMs) lack a representation of surface heat fluxes due to the mesoscale enhancement induced by subgrid-scale processes. As a result, GCMs suffer vast uncertainties in the surface energy budget that affects various phenomena on differing scales and ultimately leads to inaccurate long-range forecasting. By applying 2D and 3D cloud-resolving models to data taken during TOGA COARE, the authors attempt to provide insight via parameterizations into the functioning of 2D and 3D CRMs in approximating the mesoscale enhancement of surface heat fluxes for eventual implementation into GCMs.

The results suggest that the mesoscale enhancement by precipitating deep convection is analogous across 2D and 3D CRMs for both the sensible and latent heat fluxes. The enhancement accounts for 17% of the total sensible heat flux for both 2D and 3D CRMs. Similar results surfaced for the total latent heat flux with 18% explained by the enhancement from the 2D model and 16% from the 3D model. It seems clear that the mesoscale enhancement is apparent across various models with mean values accounting for a range of 0%–30% in the total flux (Esbensen and McPhaden 1996). However, much of the CRM data analyzed over the equatorial Pacific (e.g., Zulauf and Krueger 1997; Redelsperger et al. 2000) including the results herein indicate that the majority of mesoscale enhancement embodies the upper half of this range (15%–30%).

The representation of the gustiness based on the precipitation presented by Redelsperger et al. (2000) exhibits favorable results when evaluated against the 2D and 3D CRMs. Rainfall from deep convection brings outflows into contact with the ocean surface altering the air–sea temperature gradient through the gusty, cool air transport allowing for the modification of surface fluxes. Formulations utilizing the cloud mass fluxes will differ appreciably across various models due to the treatment of cloud microphysics and the determination of the appropriate level of calculation. Parameterizing the gustiness in terms of the cloud mass fluxes alone is insufficient in representing the mesoscale enhancement when compared to the precipitation scheme. Thus, it seems appropriate to further study coupling processes of precipitation and cloud mass fluxes with convective thresholds in order to fully recover the dynamic response of the enhancement.

Although the 3D CRM was found to have higher correlations, overall, 2D and 3D CRMs are comparable in their assessment of the mesoscale enhancement of surface heat fluxes largely due to the similar convection-induced surface gustiness and precipitation from both models. While more study is needed to deduce conclusions from results of superparameterizations, it seems sufficient to utilize the 2D CRM in the interest of saving computational costs for representing convection-induced enhancements of surface heat fluxes in GCMs.

Acknowledgments. The author (S. Guimond) wants to thank J. L. Redelsperger for the e-mail discussion on the subject and also to acknowledge use of the Ferret

program for analysis and graphics in this paper. Ferret is a product of NOAA's Pacific Marine Environmental Laboratory. (Information is available online at www.ferret.noaa.gov.) This research is partly supported by the Office of Science (BER), U.S. Department of Energy, Grants DE-FG02-02ER63483 and DE-FG02-04ER63868.

REFERENCES

Clark, T. L., W. D. Hall, and J. L. Coen, 1996: Source code documentation for the Clark-Hall cloud-scale model: Code version G3CH01. NCAR Tech. Note NCAR/TN-426+STR, 137 pp.

Esbensen, S. K., and R. W. Reynolds, 1981: Estimating monthly averaged air–sea transfers of heat and momentum using the bulk aerodynamic method. *J. Phys. Oceanogr.,* **11,** 457–465.

——, and M. J. McPhaden, 1996: Enhancement of tropical ocean evaporation and sensible heat flux by atmospheric mesoscale systems. *J. Climate,* **9,** 2307–2325.

Fairall, C. W., E. F. Bradley, D. P. Rogers, J. B. Edson, and G. S. Young, 1996: Bulk parameterization of air-sea fluxes for Tropical Ocean-Global Atmosphere Coupled-Ocean Atmosphere Response Experiment. *J. Geophys. Res.,* **101,** 3747–3764.

Godfrey, J. S., and E. J. Lindstrom, 1989: The heat budget of the western equatorial Pacific surface mixed layer. *J. Geophys. Res.,* **94,** 8007–8017.

——, and A. C. M. Beljaars, 1991: On the turbulent fluxes of buoyancy, heat and moisture at the air-sea interface at low wind speeds. *J. Geophys. Res.,* **96,** 22 043–22 048.

——, M. Nunez, E. F. Bradley, P. A. Coppin, and E. J. Lindstrom, 1991: On the net surface heat flux into the western equatorial Pacific. *J. Geophys. Res.,* **96,** 3391–3400.

——, R. A. Houze Jr., R. H. Johnson, R. Lukas, J. L. Redelsperger, A. Sumi, and R. Weller, 1998: Coupled Ocean Atmosphere Response Experiment (COARE): An interim report. *J. Geophys. Res.,* **103,** 14 395–14 450.

Grabowski, W. W., 2001: Coupling cloud processes with the large-scale dynamics using the cloud-resolving convection parameterization (CRCP). *J. Atmos. Sci.,* **58,** 978–997.

——, X. Wu, and M. W. Moncrieff, 1996: Cloud-resolving modeling of tropical cloud systems during Phase III of GATE. Part I: Two-dimensional experiments. *J. Atmos. Sci.,* **53,** 3684–3709.

——, ——, ——, and W. D. Hall, 1998: Cloud-resolving modeling of tropical cloud systems during Phase III of GATE. Part II: Effects of resolution and the third spatial dimension. *J. Atmos. Sci.,* **55,** 3264–3282.

Jabouille, P., J. L. Redelsperger, and J. P. Lafore, 1996: Modification of surface fluxes by atmospheric convection in the TOGA COARE region. *Mon. Wea. Rev.,* **124,** 816–837.

Kessler, E., 1969: *On the Distribution and Continuity of Water Substance in Atmospheric Circulations. Meteor. Monogr.,* No. 32, Amer. Meteor. Soc., 84 pp.

Kiehl, J. T., J. J. Hack, G. B. Bonan, B. A. Boville, B. P. Briegleb, D. L. Williamson, and P. J. Rasch, 1996: Description of the NCAR Community Climate Model (CCM3). NCAR Tech. Note TN-420+STR, 152 pp.

Koenig, L. R., and F. W. Murray, 1976: Ice-bearing cumulus cloud evolution: Numerical simulation and general comparison against observations. *J. Appl. Meteor.,* **15,** 747–762.

Lin, X., and R. H. Johnson, 1996: Heating, moistening, and rainfall over the western Pacific warm pool during TOGA COARE. *J. Atmos. Sci.,* **53,** 3367–3383.

Liu, W. T., 1988: Moisture and latent heat flux variabilities in the tropical Pacific derived from satellite data. *J. Geophys. Res.,* **93,** 6749–6760.

Miller, M. J., A. C. M. Beljaars, and T. N. Palmer, 1992: The sensitivity of the ECMWF model to the parameterization of evaporation from the tropical oceans. *J. Climate,* **5,** 418–434.

Mondon, S., and J.-L. Redelsperger, 1998: Study of a fair weather boundary layer in TOGA-COARE: Parameterization of surface fluxes in large-scale and regional models for light wind conditions. *Bound.-Layer Meteor.,* **88,** 47–76.

Randall, D. A., M. F. Khairoutdinov, A. Arakawa, and W. W. Grabowski, 2003: Breaking the cloud parameterization deadlock. *Bull. Amer. Meteor. Soc.,* **84,** 1547–1564.

Redelsperger, J. L., and G. Sommeria, 1986: Three-dimensional simulation of a convective storm: Sensitivity studies on subgrid parameterization and spatial resolution. *J. Atmos. Sci.,* **43,** 2619–2635.

——, F. Guichard, and S. Mondon, 2000: A parameterization of mesoscale enhancement of surface fluxes for large-scale models. *J. Climate,* **13,** 402–421.

Wallace, J. M., and P. V. Hobbs, 1977: *Atmospheric Science: An Introductory Survey.* Academic Press, 467 pp.

Webster, P. J., and R. Lukas, 1992: TOGA COARE: The Coupled Ocean—Atmosphere Response Experiment. *Bull. Amer. Meteor. Soc.,* **73,** 1377–1416.

Wu, X., and M. W. Moncrieff, 1996: Recent progress on cloud-resolving modeling of TOGA COARE and GATE cloud systems. *Proc. Workshop on New Insights and Approaches to Convective Parameterization*, Reading, United Kingdom, ECMWF, 128–156.

——, and ——, 2001: Long-term behavior of cloud systems in TOGA COARE and their interactions with radiative and surface processes. Part III: Effects on the energy budget and SST. *J. Atmos. Sci.,* **58,** 1155–1168.

——, W. W. Grabowski, and M. W. Moncrieff, 1998: Long-term behavior of cloud systems in TOGA COARE and their interactions with radiative and surface processes. Part I: Two-dimensional modeling study. *J. Atmos. Sci.,* **55,** 2693–2714.

——, W. D. Hall, W. W. Grabowski, M. W. Moncrieff, W. D. Collins, and J. T. Kiehl, 1999: Long-term behavior of cloud systems in TOGA COARE and their interactions with radiative and surface processes. Part II: Effects of ice microphysics on cloud–radiation interaction. *J. Atmos. Sci.,* **56,** 3177–3195.

Zhang, G. J., 1995: On the use of monthly mean data to compute surface turbulent fluxes in the tropical Pacific. *J. Climate,* **8,** 3084–3090.

Zulauf, M., and S. K. Krueger, 1997: Parameterization of mesoscale enhancement of large-scale surface fluxes over tropical oceans. Preprints, *22d Conf. on Hurricanes and Tropical Meteorology*, Fort Collins, CO, Amer. Meteor. Soc., 164–165.